Slow Transition of Energy Transport in High-Temperature Plasmas

K. Ida, S. Inagaki, R. Sakamoto, K. Tanaka, H. Funaba, Y. Takeiri, K. Ikeda, C. Michael, T. Tokuzawa, H. Yamada, Y. Nagayama, K. Itoh, O. Kaneko, A. Komori, O. Motojima, and LHD experimental group

National Institute for Fusion Sciences, Toki, Gifu 509-5292, Japan

(Received 3 October 2005; published 31 March 2006)

A new slow transition process for energy transport in magnetically confined plasmas is reported. The slow transition is characterized by the change between two metastable transport conditions characterized by a weak and a strong electron temperature (T_e) dependence of normalized heat flux. These two branches are found to merge at the critical T_e gradient. In metastable transport, the derivative of normalized heat flux to the T_e gradient, $\partial(Q_e/n_e)/\partial(-\nabla T_e)$, is positive, while it becomes negative during the transition phase. The time for the transition increases as the normalized T_e gradient is increased and exceeds the transport time scale characterized by the global energy confinement time.

DOI: 10.1103/PhysRevLett.96.125006 PACS numbers: 52.25.Fi, 52.50.Gj, 52.55.Hc

High-temperature plasmas, which are seen in nature or confined in laboratory experimental devices, are very often far from equilibrium. One of the noticeable features is that the observed temperature profiles are realized as a balance between the flux of energy and turbulence-driven transport. A sudden and distinctive jump in the profiles has been found, e.g., the H-mode phenomena in tokamak plasmas [1]. The concept of a profile transition has been employed in order to understand the formation and dynamics of a self-sustained radial profile in inhomogeneous plasmas [2]. The transitions in the profiles in H-mode plasmas are caused by the S-curve property (cusp-type catastrophe) in the gradient-flux relation, showing a feature analogous to the first-order phase transition [3,4]. As the second-order phase transition exists in terrestrial matter, it is possible that the other type of transition exists in the process of transport barrier formation in plasmas [4]. We here report the discovery of a new, slowly evolving transition between two transport branches that have different electron temperature (T_e) dependences, in toroidal plasmas.

Heat transport in a magnetically confined toroidal plasma is strongly governed by turbulence. The mechanism of the H-mode transition has been studied both experimentally [5,6] and theoretically [7–10]. The bifurcation of the radial electric field and the associated suppression of turbulence are the key parameters to explain the fast transition between L mode and H mode [2,7–9]. This transition mechanism appears as various phenomena such as the electric pulsation observed in the toroidal helical plasma and the internal transport barrier [11]. In parallel with these rapidly evolving phenomena, slow evolutions into the state of improved plasma confinement have also been observed in a slowly developing edge transport barrier [12] and in other confinement improved modes. Improved Ohmic confinement mode [13], counter-neutral beam injection improved mode [14], pellet enhanced performance mode [15], radiatively improved mode [16] associated with the change of density profiles without a clear fast transition. Although these improved modes associated with the slow transition are as important as the improved mode with a fast transition, the mechanism of the slow transition has been studied little because of the slow change in transport.

In general the heat flux normalized by the plasma density is a function of T_e and T_e gradients. In order study the T_e and T_e gradient dependence of electron heat transport, the normalized heat flux is scanned by changing the electron density using repetitive pellets in the Large Helical Device (LHD). The size of the repetitive pellets is 2.5 mm diameter and the volume averaged density increases by 1.6×10^{19} m^{-3} with one pellet. The speed of the pellet is 450–500 m/s and the pellets penetrate as far as from half of the plasma minor radius to the plasma center depending on the density [17]. The time evolution of the electron temperature (T_e) and the density (n_e) are measured with a 27 channel electron cyclotron emission (ECE) radiometer [18] and 14 channel FIR + CO_2 laser interferometer [19]. Figures 1(a) and 1(b) show the time evolution of the T_e and the T_e gradients during the density decay phase after the pellet injection, where the normalized heat flux increases monotonically in time by a factor of 2. Although the absolute error of the T_e gradients determined by the accuracy of the calibration of ECE radiometer is large (20%), the relative error of the T_e gradient determined by the noise level is only 1%. This relative error of the T_e gradient is small enough to discuss the 10% change in T_e gradients and their correlation with the changes in the normalized heat flux.

There are clear phases characterized by the sign of the time derivative of the T_e gradients as indicated by phases I, II, III, IV. Both T_e and the T_e gradient increase in time as the electron density decreases in phases II and IV, which is a normal characteristic of heat transport in plasma. However, in phases I and III, the T_e gradients decrease even with the increase of T_e. The change in the time derivative of the T_e gradient is abrupt (less than 0.01 sec)

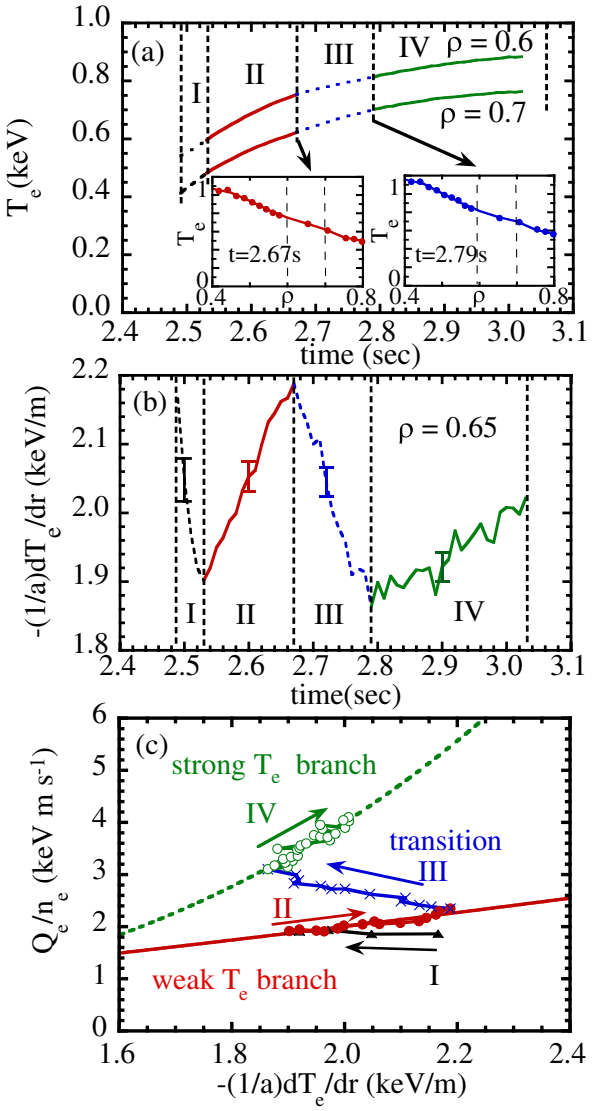

FIG. 1 (color online). Time evolution of (a) the electron temperature (T_e) at $\rho = 0.6$ and 0.7 and the normalized heat flux at $\rho = 0.65$ and (b) the T_e gradient at $\rho = 0.65$, during the T_e rise after the pellet injection. Radial profiles of T_e at the start and the end of phase III are also plotted. (c) Heat flux normalized by electron density as a function of the T_e gradient 0.02–0.06 sec (triangles), 0.06–0.17 sec (closed circles), 0.17–0.33 sec (crosses) 0.33–0.57 sec (open circles) after the pellet injection at $\rho = 0.65$.

and its value is roughly constant in time for each phase as -6.6 keV/(m/s) (in phase I), 2.2 keV/(m/s) (in phase II), -2.7 keV/(m/s) (in phase III), and 0.6 keV/(m/s) (in phase IV). This observation clearly demonstrates that the transition phase between the two metastable states is characterized by the change in the time derivative of the T_e gradient [not the T_e gradient itself as seen in the L to H-mode transition [3]].

The change in transport is more clearly presented in the relation between the heat flux normalized by the electron density and the T_e gradient as seen in Fig. 1(c). The radial profile of heat sources by neutral beam injection is calculated with the FIT code [20] based on the measured T_e and density profiles. The heat flux normalized by the electron density at $\rho = 0.65$ is determined accurately (5% error in the FIT calculation, 3% error in the electron density), because 70%–80% of the total power is deposited at $\rho < 0.65$. The energy of the NBI in LHD is high (130 keV/amu) and 4/5 of the heating power is deposited to the electrons; therefore, the ion temperature (T_i) is equal to or slightly less than the electron temperature. Because $(T_e\text{-}T_i) \propto n^{-1.6}$ and $T_e \propto n^{-0.4}$ the equilibration term normalized by the density of $(T_e - T_i)\nu_{ie}$, where ν_{ie} is the collision frequency, is almost constant in time and can be neglected in this analysis. The convective term is small enough to be neglected. There are two branches in the transport; one is characterized by a weak T_e dependence (lower branch: phase II) and the other by a strong T_e dependence (upper branch: phase IV). Phase III in Fig. 1 is the transition phase between the strong and weak T_e dependence branches. During the phase transition, the heat flux normalized by the electron density has a negative dependence on the absolute value of the T_e gradient as $\partial(Q_e/n_e)/\partial(-\nabla T_e) < 0$, which is in contrast to the normally positive dependence of $\partial(Q_e/n_e)/\partial(-\nabla T_e) > 0$ in the two transport branches. In the discharge without the perturbation of a pellet injection, the plasma is in the strong T_e dependence branch and the weak T_e dependence branch is observed after the pellet injection. The change of the T_e dependence is considered to be due to the change in the turbulence mixing state, which is discussed later.

Since the plasma temporally stays in the weak T_e dependence branch, the range of the T_e gradient change is relatively narrow during one pellet injection. However the transport in a wide range can be investigated by injecting the pellet to the plasma with different densities and Q_e/n_e. Figure 2 shows the normalized heat as a function of T_e and the T_e gradient in the weak T_e dependence branch (phase II) and in the strong T_e dependence branch (phase IV) after the pellets (12 pellets in series) are injected into the plasmas with different densities. The experimental data in phase II shows that the normalized heat flux gradually increases as the T_e and T_e gradient are increased, while that in the phase IV shows a sharp increase of the normalized heat flux. It is noted that all the experimental data points of the 12 events are connected and located along curves (data points in phase II are on a weak T_e dependence curve and data points in phase IV on a strong T_e dependence curve). The data points in the transition phase (phase III) are scattered between the weak and the strong T_e dependence curves. When the plasma is on one of the branches, both the T_e and the T_e gradient are uniquely determined for the given normalized heat flux, while they are not uniquely determined during the transition phase.

In order to investigate quantitatively the dependence of the normalized heat flux on the T_e and T_e gradient dependence, the normalized heat flux is given by $Q_e/n_e \propto T_e^{\alpha}(-\nabla T_e)^{\beta}$, where α and β are the T_e and T_e gradient

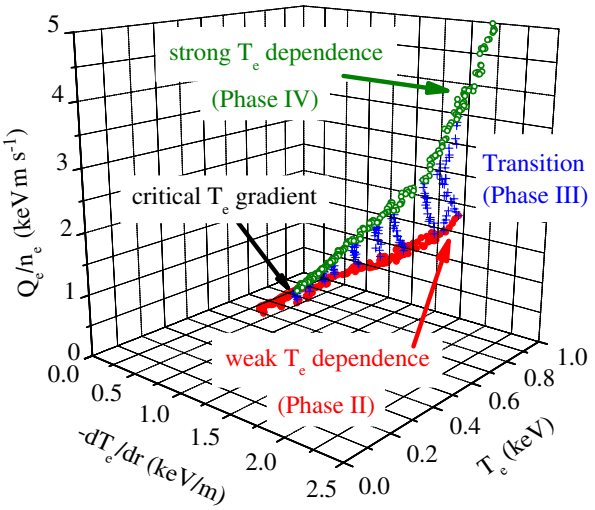

FIG. 2 (color online). Heat flux normalized by electron density as a function of electron temperature (T_e) and temperature gradient in the weak T_e dependence branch (phase II), in the transition period (phase III), and in the strong T_e dependence branch (phase IV) at $\rho = 0.65$.

dependence parameters, respectively. The difference between the Q_e/n_e measured and Q_e/n_e calculated with the parameters (α, β) are investigated in a wide range of Q_e/n_e for these two branches. Figures 3(a) and 3(b) show the contours of the square of differences between the normalized heat flux measured and that calculated, $\chi^2 = [Q_e/n_e - cT_e^{\alpha}(-\nabla T_e)^{\beta}]^2$, for various values of (α, β) in the weak and strong T_e dependence branches. The T_e dependence parameter α is $0.44(-0.23, +0.25)$ for the weak T_e dependence transport branch and $1.4(-0.4, +0.3)$ for the strong T_e dependence transport branch, while the T_e gradient dependence parameter, β, is close to unity: $0.86(-0.25, +0.25)$ and $1.1(-0.2, +0.27)$ for the weak and the strong T_e dependence branches, respectively. This strong T_e dependence is consistent with the observation in other devices when the T_e gradient is below the threshold [21]. The error bar is estimated from the range of α and β values for $\chi^2 < 1.3\chi^2_{\min}$. In this experiment, the T_e increases as the T_e gradient is increased. The colinearity between T_e and the T_e gradient causes large errors in the estimated α and β values. The $\alpha + \beta$ value is evaluated more accurately and $1.3(-0.12, +0.12)$ and $2.5(-0.24, +0.26)$ for the weak and strong T_e dependence branch, respectively.

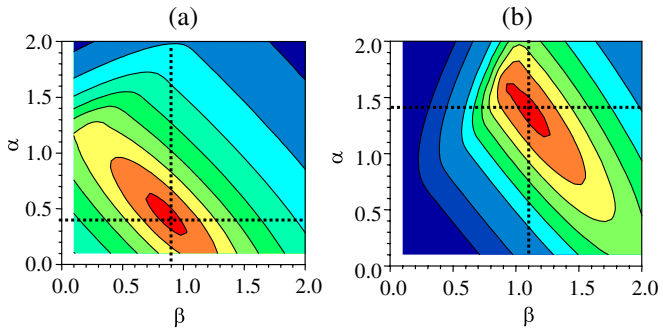

FIG. 3 (color online). The contours of the difference between the normalized heat flux measured and that calculated with the model of $cT_e^{\alpha}(-\nabla T_e)^{\beta}$ with various values of (α, β) for (a) the weak T_e dependence branch (phase II) and (b) the strong T_e dependence branch (phase IV) at $\rho = 0.65$.

The strong $(T_e, \nabla T_e)$ dependence of $\alpha + \beta = 2.3$ observed in phase VI is consistent with the gyro-Bohm-like dependence of $\alpha + \beta = 2.5$ in the collisionless regime. However, the weak $(T_e, \nabla T_e)$ dependence of $\alpha + \beta = 1.3$ observed in phase II is much weaker than the gyro-Bohm dependence and it can be understood by taking account of the influence of a zonal flow. When zonal flows coexist with drift wave turbulence, the turbulence transport coefficient is strongly influenced by the damping rate of the zonal flow and deviates from the gyro-Bohm dependence [22]. The $\alpha + \beta$ value depends on fluctuation levels and, when the collisional process governs the damping of zonal flow, it can be 1.5, which is consistent with the measurements in phase II. Direct measurements of zonal flow in LHD are necessary to confirm this hypothesis.

As seen in Fig. 2, the two transport branches discussed above merge as T_e and the T_e gradient become small enough, which is defined as the critical T_e gradient. Below the critical T_e gradient, only the weak T_e dependence branch, which becomes the upper branch in turn, is observed. In the discharges without the perturbations of pellet injection, the plasma remains in only the upper branches (the strong T_e dependence branch above the critical T_e gradient and the weak T_e dependence branch below the critical T_e gradient) and the heat transport changes its T_e dependence at this critical T_e [23]. Since this critical T_e gradient becomes higher towards the plasma core, the transition between the weak and the strong T_e transport branches is observed typically at $\rho = 0.6$–0.8. As the normalized heat flux is increased, the layer where the transition is observed extends to the plasma core.

The transition between the two transport branches is relatively slow compared with the transition from the L mode to the H mode or from ion root to electron root, where the bifurcated radial electric field is the key mechanism. The time for the transition defined as the time for the plasma transport to move from one branch to the other branch can be obtained from the time interval of two abrupt changes of the time derivative of the T_e gradient. Figure 4(a) shows the transition from a weak T_e dependence branch to a strong T_e dependence branch after the pellet is injected to the plasma at different T_e gradients. As the T_e gradient approaches to the critical T_e gradient, the transition is dominated more by the change in the T_e gradient rather than by the change in normalized heat flux. The change of the characteristics of transition is due to the change of the time for transition, since the change of normalized heat flux is determined by the density decay after the pellet, which is governed by the particle transport

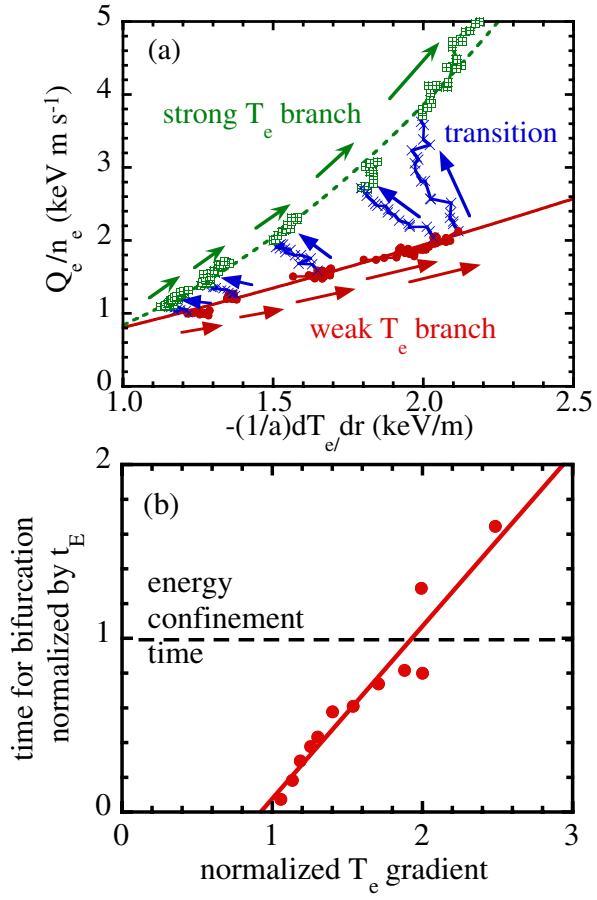

FIG. 4 (color online). (a) Heat flux normalized by electron density as a function of electron temperature (T_e) gradient at $\rho = 0.65$ after each pellet injection. (b) Time for the transition (phase III) normalized by the energy confinement time as a function of the T_e gradient normalized by the critical T_e gradient.

time scale. As shown in Fig. 4(b), the time for the transition depends on the T_e gradient and it increases linearly as the ratio of the T_e gradient to the critical T_e gradient increases. The time for the transition can be as large as the global energy confinement time, which is in contrast to the fast transition as observed in the L-H transition and electric pulsation where the bifurcation of the radial electric field plays a role. The different T_e dependence of the transport suggests that the dominant turbulence differs between these two branches. The slow transition between these two branches is due to the existence of a mixed state of two dominant turbulences.

The observation of two distinct turbulent states casts illumination on the understanding of turbulent transport. Many kinds of instabilities in the range of the drift wave frequency have been studied in toroidal plasmas [24]. Recently it has been pointed out that competition among different instabilities affects the saturation of turbulence [25,26]. Because of the nonlinear coupling between different types of turbulence, slow transitions between two states with different dominant turbulence types are theoretically predicted [25]. The identification of the two transport branches in the LHD provides a manifestation of these theoretical analyses and stimulates further theoretical study on nonlinear competition among the different types of turbulence. In conclusion, we have identified a new transition process between two metastable transport conditions; one is $Q_e/n_e \propto T_e^{0.4}(-\nabla T_e)^{0.9}$ and the other is $Q_e/n_e \propto T_e^{1.4}(-\nabla T_e)^{1.1}$. The time for the transition characterized by $(Q_e/n_e)/\partial(-\nabla T_e) < 0$ increases as the normalized T_e gradient is increased and exceeds the transport time scale characterized by the global energy confinement time.

We would like to thank the technical staff for their effort to support the experiment in LHD. One of authors (K. I.) acknowledges discussion with Professors S.-I. Itoh and A. Fukuyama. This work is partly supported by a Grant-in-Aid for Scientific research (No. 15206106) and the Grant-in-Aid for Specially-Promoted Research (No. 16002005) of MEXT Japan. This work is also partly supported by NIFS05LUBB510.

[1] F. Wagner *et al.*, Phys. Rev. Lett. **49**, 1408 (1982).
[2] K. Itoh, S.-I. Itoh, and A. Fukuyama, *Transport and Structural Formation in Plasmas* (IOP, Bristol, 1999).
[3] A. E. Hubbard *et al.*, Plasma Phys. Controlled Fusion **44**, A359 (2002).
[4] V. B. Lebedev *et al.*, Phys. Plasmas **4**, 1087 (1997).
[5] R. J. Groebner *et al.*, Phys. Rev. Lett. **64**, 3015 (1990).
[6] K. Ida *et al.*, Phys. Rev. Lett. **65**, 1364 (1990).
[7] S.-I. Itoh *et al.*, Phys. Rev. Lett. **60**, 2276 (1988).
[8] K. C. Shaing *et al.*, Phys. Rev. Lett. **63**, 2369 (1989).
[9] H. Biglari *et al.*, Phys. Fluids B **2**, 1 (1990).
[10] P. H. Diamond *et al.*, Phys. Rev. Lett. **72**, 2565 (1994).
[11] A. Fujisawa *et al.*, Phys. Rev. Lett. **81**, 2256 (1998).
[12] R. A. Moyer *et al.*, Plasma Phys. Controlled Fusion **41**, 243 (1999).
[13] F. X. Soldner *et al.*, Phys. Rev. Lett. **61**, 1105 (1988).
[14] O. Gehre *et al.*, Phys. Rev. Lett. **60**, 1502 (1988).
[15] B. J. D. Tubbing *et al.*, Nucl. Fusion **31**, 839 (1991).
[16] J. Ongena *et al.*, Phys. Scr. **52**, 449 (1995).
[17] H. Yamada *et al.*, Fusion Eng. Des. **69**, 11 (2003).
[18] K. Kawahata *et al.*, Rev. Sci. Instrum. **74**, 1449 (2003).
[19] K. Tanaka *et al.*, Rev. Sci. Instrum. **75**, 3429 (2004).
[20] S. Murakami *et al.*, Fusion Technol. **27**, 256 (1995).
[21] F. Imbeaux *et al.*, Plasma Phys. Controlled Fusion **43**, 1503 (2001).
[22] P. H. Diamond *et al.*, Plasma Phys. Controlled Fusion **47**, R35 (2005).
[23] J. Miyazawa *et al.*, Plasma Phys. Controlled Fusion **47**, 801 (2005).
[24] W. M. Tang, Nucl. Fusion **18**, 1089 (1978).
[25] S.-I. Itoh and K. Itoh, Plasma Phys. Controlled Fusion **43**, 1055 (2001).
[26] C. Holland *et al.*, Phys. Plasmas **11**, 1043 (2004).